Mine Water and the Environment (2025) 44:55–64
https://doi.org/10.1007/s10230-025-01030-7

TECHNICAL ARTICLE

Exploring Spatiotemporal Trends in Piezometer Network Data Using Self-Organizing Maps

Emily Mee[1] · **Roger Beckie**[1]

Received: 28 June 2024 / Accepted: 31 January 2025 / Published online: 18 February 2025

Abstract
Large piezometer networks are implemented at mine sites for geotechnical and environmental monitoring. Groundwater head time series from these networks contain valuable information about aquifer stresses and hydraulic connections. Machine learning methods can efficiently extract information from large volumes of head data but are not yet common practice. To illustrate the utility of machine learning in a practical context, we use the self-organizing map (SOM) method to extract patterns from groundwater head time series for 85 piezometers at the Red Chris Mine in northern Canada. Aquifer response and hydraulic connectivity are uncertain at the site due to changing stresses and geological heterogeneity. We demonstrate the influence and choice of the map size hyperparameter. 'Small maps' provide insight on aquifer-scale hydraulic behavior and 'large maps' can highlight local anomalies like borehole leakage and repair. We evaluated SOM output using site-specific knowledge of geology and groundwater flow. The SOM results reveal spatiotemporal trends that were not readily apparent from previous site characterization studies.

Keywords Groundwater · Machine learning · Water level · Cluster analysis · SOM · Aquifer characterization

Introduction

Groundwater is an integral component of the hydrologic cycle and an important source of water for people and the environment. Groundwater is difficult to characterize and manage because the subsurface environment is heterogeneous and data is sparse. Most types of data are only available for a small portion of the subsurface since direct observations are expensive and time consuming to collect. It is also difficult to estimate conditions at unsampled locations since geological materials are often heterogeneous. Spatial data sparsity is an ongoing challenge, but sensors and telemetry are now commonly used to collect high-frequency (e.g., hourly) groundwater head time series. Head variation is a function of stresses and hydraulic properties across the aquifer system. It can be difficult to interpret and extract information from head time series data. Visual interpretation and manual inspection are possible for small networks (Butler et al. 2021), but clustering can facilitate interpretation of larger datasets. We use the unsupervised self-organizing map (SOM) method to identify spatiotemporal patterns for 85 piezometer head time series from a multi-layered aquifer system at Red Chris Mine. We evaluate the influence of user chosen map size. We also compare the SOM results with existing knowledge of the site to determine the unique contributions of machine learning.

Clustering of head time series can be used to identify spatial zones with distinct hydrogeological characteristics and behavior (Clark 2022; Naranjo-Fernández et al. 2020; Rinderer et al. 2019; Sartirana et al. 2022). The SOM method has become increasingly popular for clustering hydrological data due to its intuitive implementation and straightforward visual output (Clark et al. 2020; Kalteh et al. 2008). Clark et al. (2020) provides a detailed description of the SOM method and guidance for implementation in water resources research and engineering. Hyperparameter selection and the interpretability of results are barriers for practical use of machine learning. Map size is an important hyperparameter of the SOM method, but it cannot be optimized with a single mathematical expression, there is no overall preferred method for map size selection, and many

✉ Emily Mee
emee@eoas.ubc.ca

Roger Beckie
rbeckie@eoas.ubc.ca

[1] Department of Earth, Ocean, and Atmospheric Sciences, University of British Columbia, Vancouver, BC, Canada

papers do not explain their rationale for choice of map size (Clark et al. 2020). We discuss the influence of map size and our map size selection for a practical case.

Successful machine learning applications require integration with subject-matter expertise (Dramsch 2020). Interpretation of machine learning results can be difficult since the relationships between variables do not necessarily have a physical meaning. The Red Chris Mine is representative of typical mine sites with dense piezometer monitoring networks around key infrastructure. It is also a compelling example because there is a wealth of site-specific knowledge to support interpretation and uncertainty resulting from the complex groundwater environment.

The Red Chris Mine groundwater system has multiple aquifers layers comprising heterogeneous glaciofluvial, glaciolacustrine, till, and colluvial soils. Head time series are feature-rich due to seasonal changes in climate and groundwater pumping. Numerous groundwater characterization studies have been undertaken to support environmental assessment and operational decision making, but there is remaining uncertainty. Hydraulic connections between aquifer units and variations within the intermediate aquifer are uncertain. These features will impact the system response to long-term groundwater pumping and potential pathways for mine-impacted water. The interpretation of SOM clustering results focuses on these features of practical importance.

In the rest of this paper, we first describe the aquifer system at Red Chris Mine and the piezometer time series data. We then briefly describe the SOM method and how we applied it to the head time series data. Then, we introduce the SOM results, discuss map size selection, and finally, interpret spatiotemporal patterns in the clustering results.

Methods

Aquifer System and Piezometer Head Time Series

The data for this study were collected in the North Valley area at Red Chris Mine, where pumping wells supply water for mine operations and piezometers are used to monitor head (locations are shown in Fig. 1). Sediments in the valley bottom are up to 125 m thick and previous site characterization studies have identified a sequence of aquifer and aquitard units. The conceptual model of aquifer and aquitard units is shown Fig. 2 and the number of piezometers in each

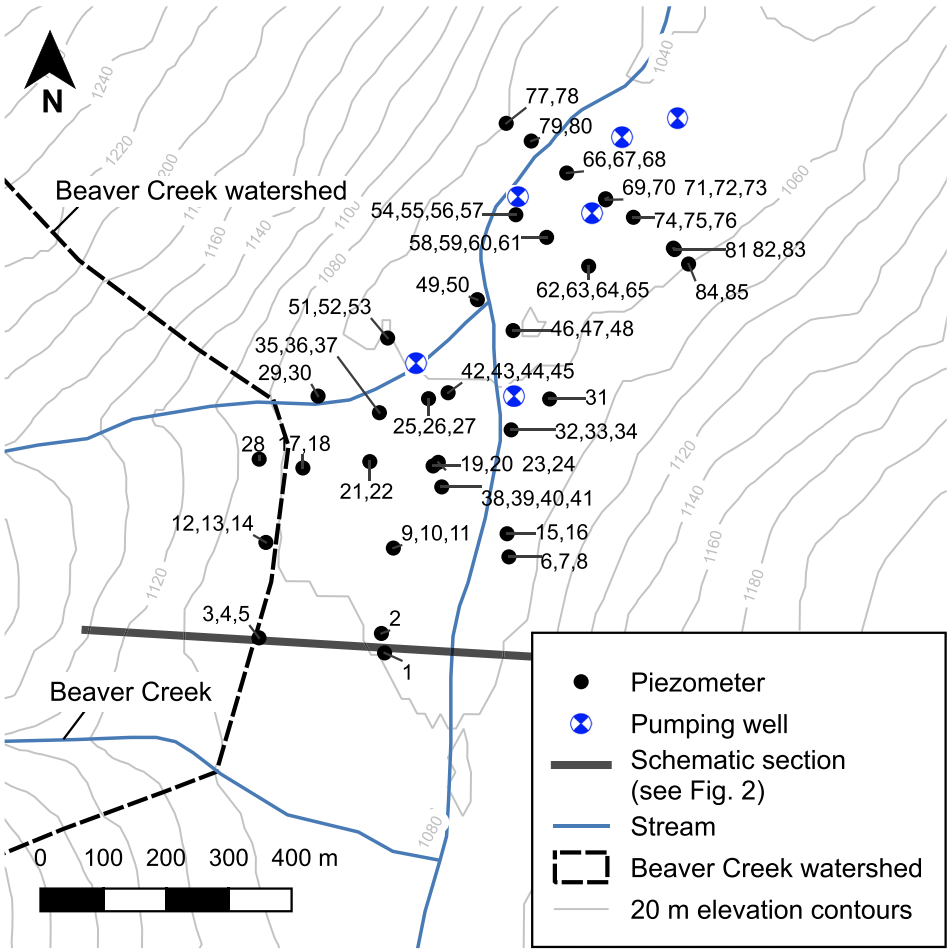

Fig. 1 Piezometer and pumping well locations in the North Valley area at Red Chris Mine (456700E, 6401000N)

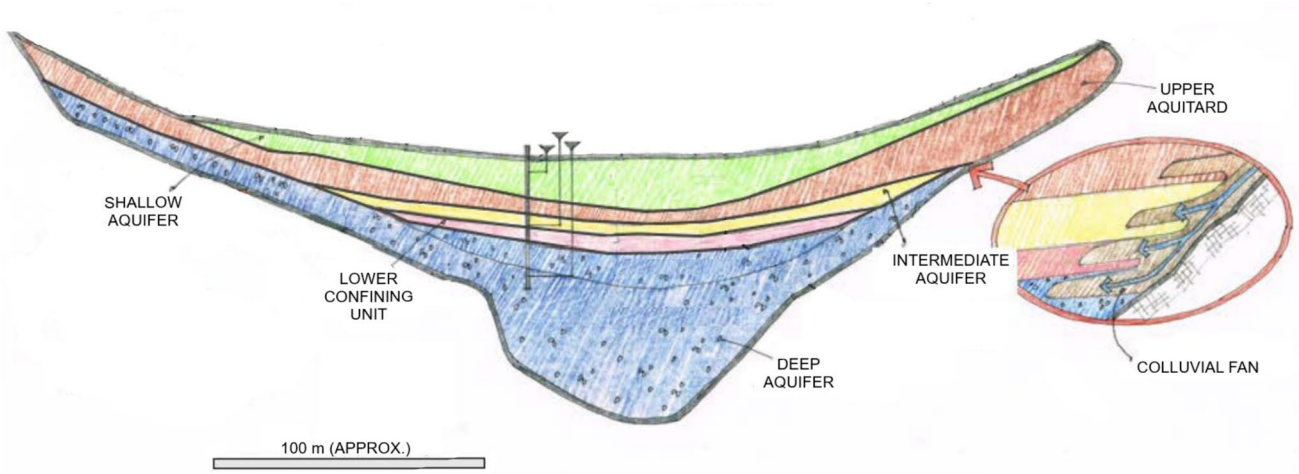

Fig. 2 Modified from Sauve et al. (2023). Schematic section of interpreted hydrostratigraphic units in the North Valley. The colours correspond to the different units and a description of each unit is provided in Table 1. Inset shows potential hydraulic connection between units at the valley wall

unit is summarized in Table 1. This conceptualization of the groundwater system was developed by practitioners using standard site characterization methods and drill hole lithology, geophysical survey, and head data (Sauve et al. 2023). The subsurface conditions are complex with heterogeneous sediments deposited during cycles of glacial advance and retreat (Sauve et al. 2023). The hydraulic connections between aquifer units and head response within the intermediate aquifer are uncertain due to the heterogeneity of glacial sediments.

In the North Valley, groundwater generally flows northeast toward the Klappan River, located ≈ 10 km downgradient. Groundwater head in the shallow aquifer is generally 0–5 m below ground surface and is relatively unaffected by deep aquifer pumping (Newcrest Red Chris Mining Limited 2023). Flowing artesian heads are observed in the intermediate aquifer and deep aquifer when deep aquifer pumping is low or inactive. Up to 40 m of drawdown have been observed at some locations in the deep aquifer and 3–13 m of drawdown have been observed at locations in the intermediate aquifer during pumping (Newcrest Red Chris Mining Limited 2023). Muted response in the intermediate aquifer suggests this unit is hydraulically isolated from the deep aquifer to some degree. Drawdown in the intermediate

Table 1 Interpreted hydrostratigraphic units in the North Valley[a]

Interpreted hydrostratigraphic unit	Geological description	Piezometric elevation	Average hydraulic conductivity (m/s)	Piezometers with available data
Shallow aquifer	Colluvium, alluvium, glaciofluvial, and occasional glaciolacustrine and ablation till	0–5 m below ground surface, with limited response to deep aquifer pumping	9×10^{-5} (n = 14)	14
Upper aquitard	Ablation till, basal till, occasional glaciolacustrine and colluvium	–	No data available	21
Intermediate aquifer	Glaciolacustrine sand, occasional packages of laminated silt/clay	1–14 m above ground surface, reduced up to 13 m during deep aquifer pumping	7×10^{-6} (n = 22)	26
Lower confining unit	Glaciolacustrine sand with packages of laminated silt/clay	–	Limited data available	8
Deep aquifer	Glaciofluvial, some glaciolacustrine, basal till	Near or above ground surface, reduced up to 40 m during deep aquifer pumping	8×10^{-5} (n = 30)	16
Bedrock	Sandstone, siltstone, conglomerate	No data available	2×10^{-9} (n = 9)	–

[a]Modified from Table 9.2–1 in Newcrest Red Chris Mining Limited (2023)

aquifer varies between different piezometers based on proximity to the deep aquifer pumping wells and geological heterogeneity (Newcrest Red Chris Mining Limited 2023).

Groundwater head data are available for 85 piezometers installed at various locations and depths in the aquifer system. Piezometer head time series are shown in Fig. 3a. Vibrating wire piezometers were installed using the grout backfill method (Mikkelsen 2002). Head measurements are recorded every 6 h. The piezometer monitoring network was expanded in 2020, so a two-year study period from October 1, 2020 to October 1, 2022 was selected to maximize the number of piezometer locations.

The head time series are feature-rich due to seasonal changes in groundwater pumping and recharge. Total daily groundwater extraction for the North Valley pumping wells is shown in Fig. 3b. Pumping rates vary seasonally depending on surface water availability. Pumping rates are greater in the winter months when surface water is largely frozen and less in the spring and summer when surface water is unfrozen.

The average annual precipitation is estimated to be 552 mm, of which 54% falls as rain and 46% falls as snow (Newcrest Red Chris Mining Limited 2023). Total annual precipitation was 731 mm in 2020 (Newcrest Red Chris Mining Limited 2021), 490 mm in 2021 (Newcrest Red Chris Mining Limited 2022), and is uncertain in 2022 due to instrumentation error (Newcrest Red Chris Mining Limited 2023). Seasonal groundwater recharge is expected to occur

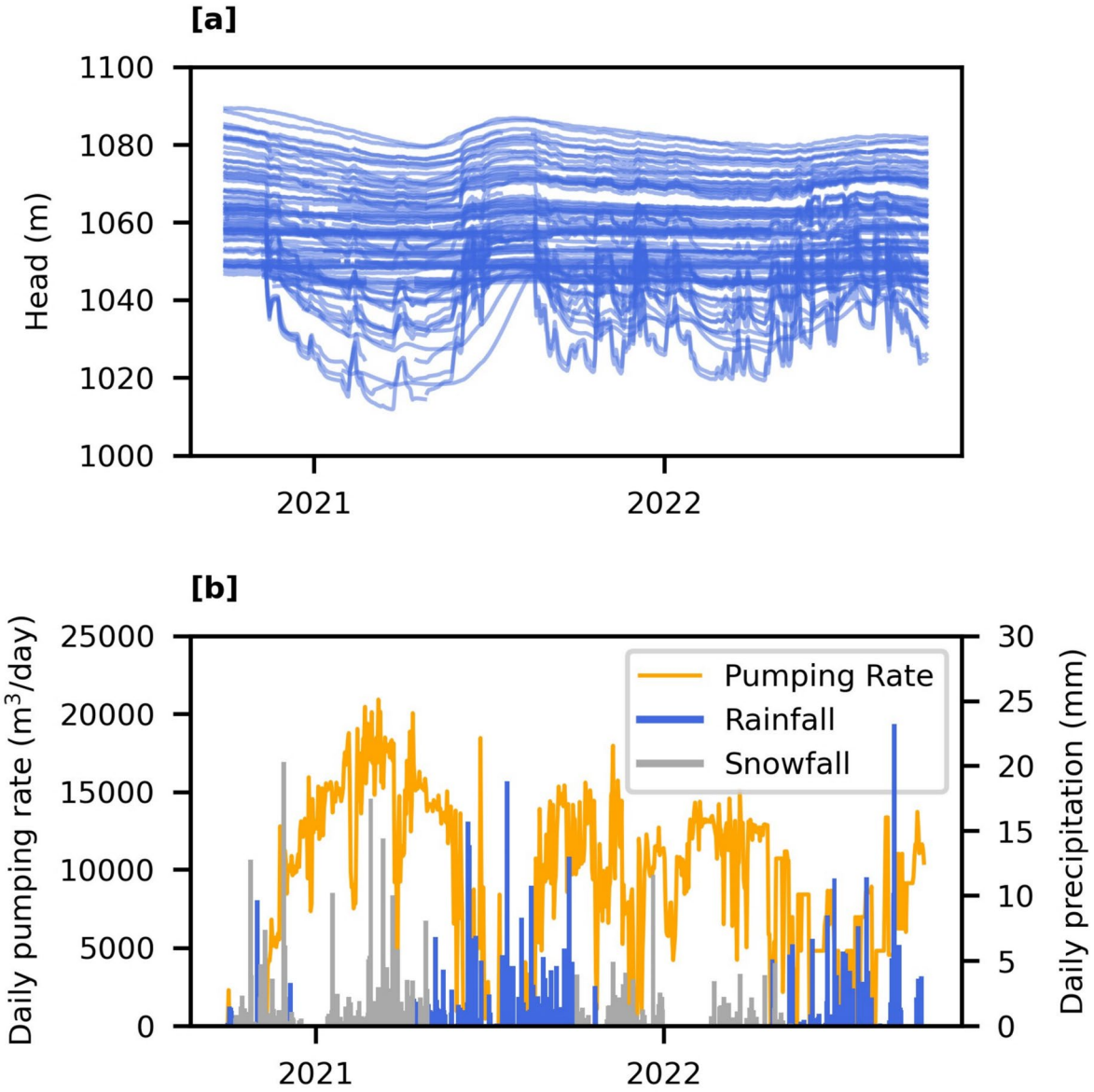

Fig. 3 **a** Daily piezometer head measurements and **b** deep aquifer pumping rate and precipitation

during periods of snowmelt and rainfall. Daily rainfall and snowfall data are shown in Fig. 3b. Heads increase in spring and summer months as groundwater pumping decreases (Fig. 3). Heads may also increase in the spring and summer due to seasonal recharge, but this potential trend is obscured by responses to groundwater pumping.

The influence of the Beaver Creek watershed on system behavior is uncertain, but this watershed is conceptualized to recharge the aquifer units. Figure 1 shows where the Beaver Creek watershed (7.8 km^2) drains into the North Valley near the southern end of the piezometer network. A large colluvial fan is observed where Beaver Creek drains into the North Valley. Discontinuous lenses of coarse-grained materials have been encountered in this area during previous subsurface investigations, but the continuity and hydraulic influence of these fan deposits are not well understood.

Self-organizing Map Analysis

All data was processed and analysed using Python Version 3.9 (Python Software Foundation 2022). There are some gaps in the head data where erroneous readings were removed or dataloggers were disconnected or malfunctioned. Gaps in the time series are typically less than 2 weeks long and the largest gap was ≈ 3 months. Data with gaps can be accommodated in SOM analysis with random initialization. For this dataset with relatively small gaps, we filled the gaps by linear interpolation to allow SOM analysis with principal component initialization. Time series were resampled from the 6-h interval to daily average values. Each time series used in analysis included 731 daily head values. To facilitate comparison of heads at different locations, the temporal average of each head time series was subtracted to produce zero-mean time series. The time series were not rescaled since the magnitude of head change provides meaningful information about hydraulic behavior.

The SOM method was implemented in Python using the MiniSom package (Vettigli 2018). The SOM algorithm creates map times series as weighted combinations of each input time series (Fig. 4). We initialized the map time series using a linear combination of the first two principal components of the dataset. An iterative training process is used to update the weights and positions of the map time series within the map grid. The map time series are positioned at nodes on a map grid with more closely related time series closer together (Kohonen 2001). To facilitate this organization of map patterns, hexagonal map grids are usually preferred over rectangular grids which favor the horizontal and vertical directions (Kohonen 2001). A hexagonal grid topology was used for this study.

SOM training and clustering are achieved by identifying the best matching unit (BMU) for each input time series (each piezometer). For each piezometer, the closest

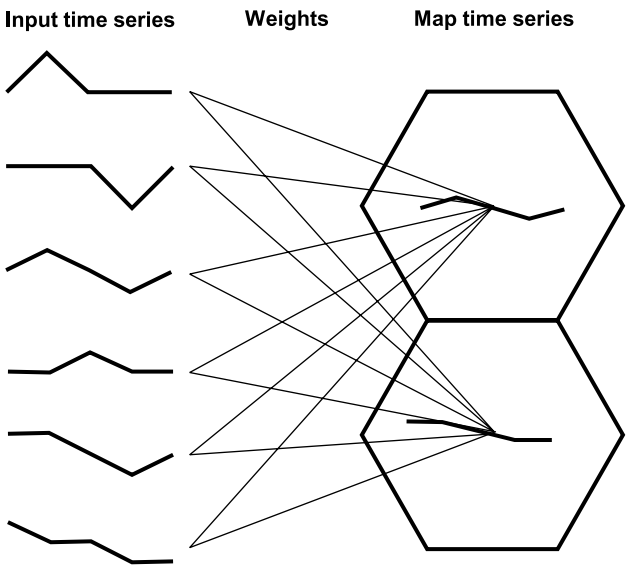

Fig. 4 Schematic of weights connecting input time series to map time series in SOM analysis

(Euclidean distance) map time series is referred to as its BMU. Since the number piezometer time series is greater than the number of map time series, multiple piezometers share the same BMU. In this study, 'BMU cluster' refers to a collection of piezometers that share the same BMU.

At each step in the training process, one piezometer time series is presented and the best matching map time series is identified. The map time series of the BMU and its neighbors are then shifted toward the piezometer time series. Map time series positioned close to the BMU are shifted more and map time series further from the BMU are shifted less. The Gaussian neighbourhood function in MiniSom was used to determine the size of the shift for each map time series based on proximity to the BMU. At the start of training, the radius of the neighborhood function must be sufficiently large for the map to become globally ordered (Kohonen 2001). An initial radius value of 1.0 was used and the asymptotic decay function in MiniSom was used to decrease the radius of the neighbourhood function throughout the training process. The learning rate η also controls the size of the shift of the map time series at each step. An initial learning rate of 0.2 was used and the asymptotic decay function was used to decrease the learning rate η throughout the training process.

The user specifies the map size (number of grid nodes) and shape (ratio of grid length to width). Map size selection is not straightforward since the SOM algorithm has two competing goals. Quantization error and topographic error are commonly used to quantify these goals (Clark et al. 2020; Kohonen 2001). The first goal is to create map patterns that closely fit the data. Quantization error is the distance between the data and their best matching map pattern.

As the number of map patterns increases, quantization error decreases as the map patterns become more similar to the data patterns. The second goal is to position the map patterns so that they closely imitate the topology of the dataset. Topographic error is the fraction of data for which the first- and second-best matching map patterns are not adjacent on the map grid. As the number of map patterns increases, topographic error generally increases as similar map patterns become more spread out in the map grid. Map size and shape are commonly selected by minimizing error measures or by visually or graphically comparing outputs for different map sizes (Clark et al. 2020). In general quantization and topographic error cannot both be minimized, and trial and error can be time consuming and subjective. We use error measures as a guide to select a range of different map sizes.

We created a series of maps to assess the effect of map size and shape on clustering results. Map width and length were varied from 2 to 9 to create 64 maps of different sizes and shapes. The number of map time series (m) ranges from 4 (2×2) to 81 (9×9). Quantization and topographic error measures were used to select eight maps for interpretation. For the selected maps, we compared the SOM clusters to the conceptual model developed through previous site characterization work. Practitioners have previously identified which piezometers are installed in each of the interpreted hydrostratigraphic units (Table 1). This existing classification was used to help identify SOM clusters that correspond to the different aquifer units. We also investigated the differences between 'small' ($m < 25$) and 'large' ($m > 25$) map sizes. This distinction between small and large maps is subjective and will vary for other applications. In general, a map can be considered 'large' if it has many nodes that reveal fine details in the data but is somewhat challenging or tedious to interpret.

Results and Discussion

The SOM output with grid length of 5 and grid width of 2 (5×2) is presented in Fig. 5. Each BMU in the map grid represents a cluster of piezometer time series and each BMU time series is an average of the corresponding piezometer time series. In the SOM output, we can identify groups of BMUs (A, B, and C) that approximately correspond to the deep aquifer, intermediate aquifer, and shallow aquifer units. The Group C time series show little to no response to pumping. Group C includes 13 (out of 14) piezometers installed in the shallow aquifer unit and 10 (out of 21) piezometers installed in the upper aquitard. The Group A time series show 10–30 m of head drawdown in response to deep aquifer pumping. Group A includes all 16 piezometers installed in the deep aquifer unit. Group B includes piezometers installed in the intermediate aquifer (20), upper aquitard (11), and lower confining unit (3). BMU 5, 8, and 10 provide new insight into the behavior of the intermediate aquifer and hydraulic connection between the aquifer units. The potential physical interpretation of these SOM clusters is discussed below.

Map Size Selection

To assess the influence of map size, 64 maps of varying size and shape were evaluated using quantization error and topographic error measures. Quantization error is strongly correlated with map size (Spearman $R = -0.92$, p value < 0.001) (Fig. 6a) and topographic error is moderately correlated with map size (Spearman $R = 0.50$, p value < 0.001) (Fig. 6b). There is more spread in the topographic error values than the quantization error values,

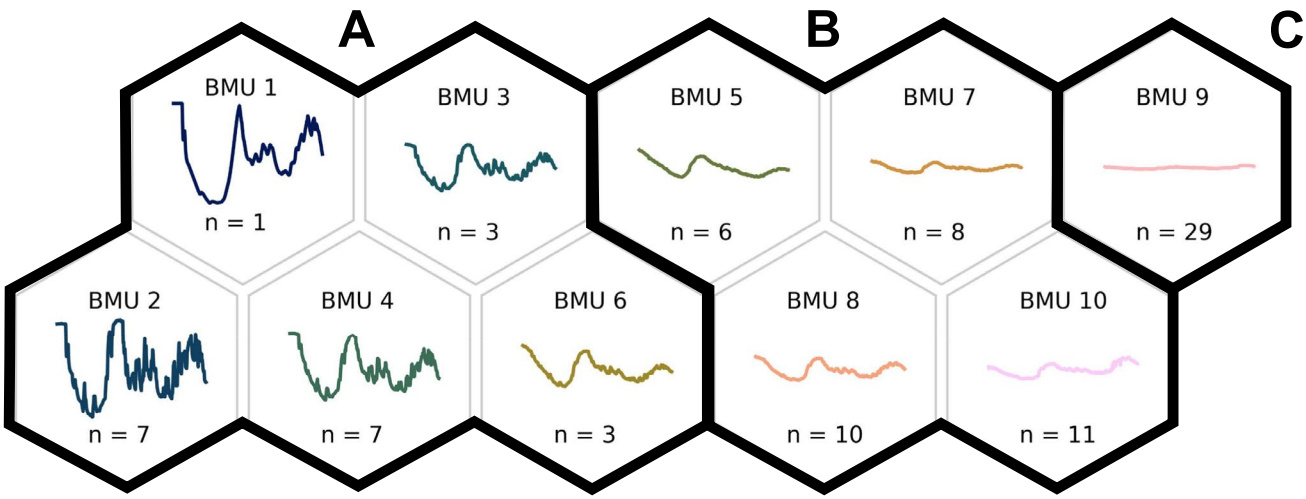

Fig. 5 5×2 SOM output with 10 best matching units (BMUs). Each cell shows the number (n) and average of the individual piezometer time series in the BMU cluster

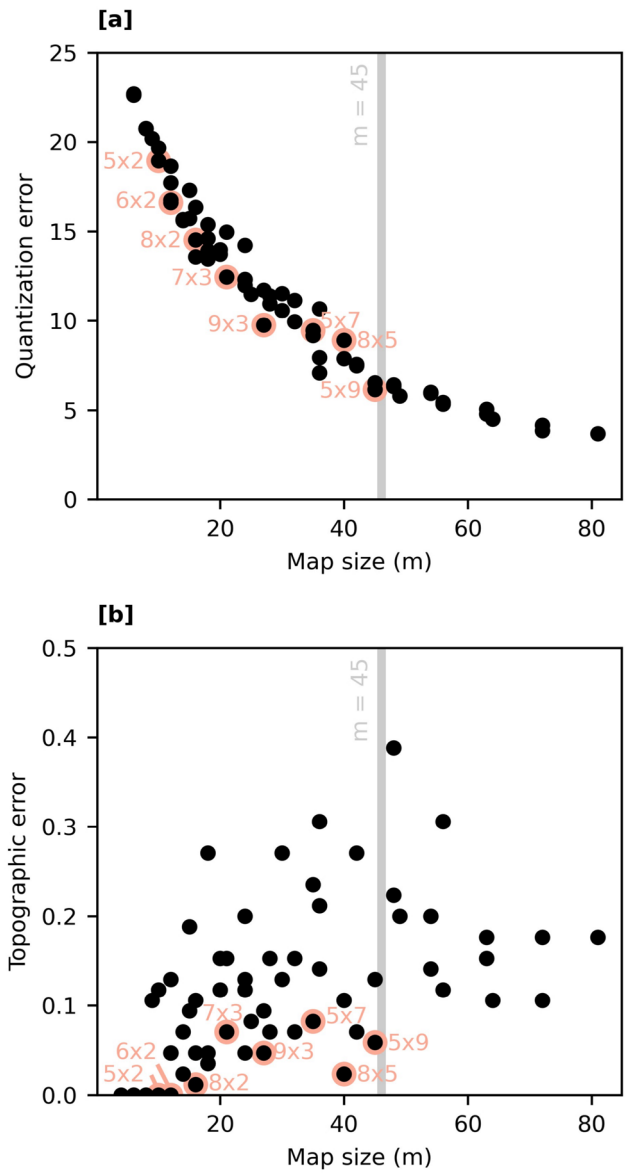

Fig. 6 Variation in **a** quantization error and **b** topographic error with map size (m = number of map time series)

which indicates that topographic error is more strongly influenced by map shape (ratio of map length to width). We observe the known trade-off where quantization error decreases and topographic error increases with increasing map size. We selected eight map sizes with a range of quantization and topographic error values. The selected maps are labelled in Fig. 6a and b. There is relatively little change in quantization error and topographic error for map sizes greater than m = 45, so a 5 × 9 map (m = 45) was the maximum size considered for interpretation. For maps with a similar size, topographic error varies depending on map shape. We selected map shapes that approximately minimize topographic error.

The eight selected maps were investigated visually and graphically to understand spatiotemporal patterns. In the smallest 5 × 2 and 6 × 2 maps, hydraulic response in the intermediate aquifer is primarily represented by four BMUs. In the larger maps (8 × 2, 7 × 3, 9 × 3, 5 × 7, 8 × 5, and 5 × 9), piezometers in the intermediate aquifer are spread over a larger number of BMUs. Relatively large map sizes are commonly used in SOM applications, particularly for large datasets and two stage clustering where the SOM method is used in the first stage and k means or another clustering method is used in the second stage. The most used heuristic for SOM map size selection is $m = 5\sqrt{n}$, where n is the number of data (Vesanto and Alhoniemi 2000). This heuristic formula suggests a map size of m ≈ 46 for this dataset. We find that the much smaller 5 × 2 map (m = 10) is optimal for simplified visualization and interpretation of general trends in the aquifer system. Larger maps support interpretation of more localized trends and are briefly discussed below. These results demonstrate the value of exploring different map sizes.

Interpretation of Spatiotemporal Patterns

The 5 × 2 map has four BMU clusters in Group B (Fig. 5). Figure 7 shows the spatial distribution of the BMU clusters in Group B. The BMU 7 cluster has a limited response to deep aquifer pumping. Piezometers matched to BMU 7 are spread out along the length of the valley. These piezometers are installed in the upper aquitard or near the top of the intermediate aquifer. Limited response at these locations is likely due to the vertical (and sometimes lateral) distance to the deep aquifer. Head changes in the intermediate aquifer are known to vary based on proximity to the deep aquifer pumping wells (Newcrest Red Chris Mining Limited 2023). This BMU cluster is consistent with the existing conceptual understanding of the aquifer system.

The BMU 8 cluster has a larger amplitude response to deep aquifer pumping than BMU 7 and BMU 10. There are four piezometers (piezometers 67, 71, 72, and 79 shown in Fig. 1) matched to BMU 8 near the north end of the monitoring network. The larger drawdown and recovery at these locations is mostly likely due to close lateral proximity to the deep aquifer pumping wells. It is also possible that there is a greater hydraulic connection between the intermediate aquifer and deep aquifer units where these piezometers are located.

Near the center of the monitoring network, there is a cluster of piezometers matched to BMU 10. The BMU 10 cluster has a lower amplitude response to deep aquifer pumping than BMU 8, even though the piezometers are in close lateral proximity to the deep aquifer pumping wells. South of the BMU 10 cluster, there are six more piezometers matched to BMU 8. These locations show a larger

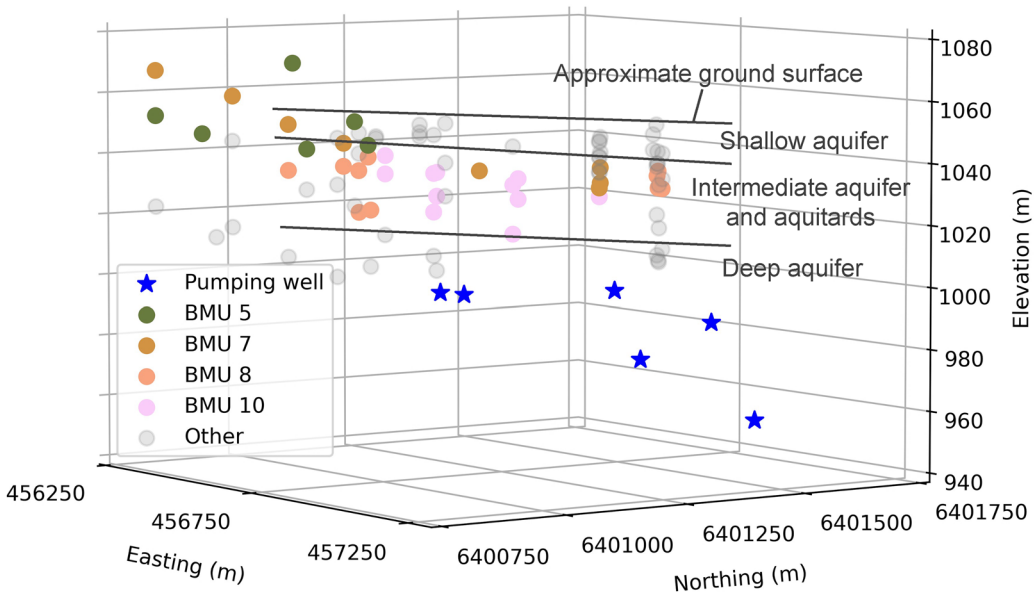

Fig. 7 Cross-sectional view (looking northwest) of SOM clusters for the intermediate aquifer. Each point represents a piezometer with a corresponding head time series

amplitude response to deep aquifer pumping even though they are further from the pumping wells. The transition from BMU 10 with poor hydraulic connectivity to BMU 8 with greater hydraulic connectivity suggests geological heterogeneity at the scale of the network.

Coarse-grained colluvial fan deposits have been encountered in the subsurface where the Beaver Creek watershed drains into the North Valley (Fig. 1). The SOM results suggest that the hydraulic connection is greater between the deep aquifer and the intermediate aquifer near the Beaver Creek outlet. The transition from BMU 8 to BMU 10 may indicate that sediments become more fine-grained further away from the fan apex. BMU 10 may represent a lower hydraulic conductivity zone within the intermediate aquifer. These zones with different hydraulic connectivity can be identified from patterns in each of the eight map sizes but are more easily distinguished in smaller maps with fewer patterns to compare. This spatial zonation in the intermediate aquifer was not readily apparent from previous site characterization work, so this is a potential new insight revealed by SOM clustering. Site characterization work typically depends on practitioner's judgement and ability to discern patterns in data, which is particularly challenging for heterogeneous environments. Practitioners described the intermediate aquifer as heterogeneous and did not clearly describe any spatial variations in hydraulic properties. The SOM clustering results suggest potential spatial variation in the intermediate aquifer that was obscured by the more obvious heterogeneity.

Piezometers at the south end of the monitoring network are matched to BMU 5. The BMU 5 cluster shows a greater decrease in head over the two-year period (Theil-Sen slope = − 2.3 m per year) compared to the BMU 8 cluster (Theil-Sen slope = − 0.2 m per year). Precipitation was above average in summer 2020 and early 2021 (Newcrest Red Chris Mining Limited 2021, 2022) and below-average in fall 2021 and 2022 (Newcrest Red Chris Mining Limited 2022, 2023). Decreasing precipitation and groundwater recharge over the two-year study period may explain the overall decrease in head observed in BMU 5. Recharge may have a greater influence at the BMU 5 piezometers because they are further from the deep aquifer pumping wells and/or closer to the outlet of the Beaver Creek watershed than the BMU 8 piezometers. This result supports the notion that the Beaver Creek fan recharges the intermediate aquifer (Newcrest Red Chris Mining Limited 2023). In previous studies, practitioners have not distinguished head changes due to variable recharge from head changes due to variable pumping. Therefore, the head change associated with variable recharge has not been quantified. The difference in overall trend between the BMU 5 and BMU 8 clusters suggests that climate and recharge variation may results in head changes of 5 m or more over a two-year period.

The 5 × 2 map provides insights into aquifer-scale hydraulic behavior. More localized hydraulic behavior could be identified within the larger maps. The 7 × 3, 9 × 3, 5 × 7, 8 × 5, and 5 × 9 maps have a BMU cluster that highlights the distinct hydraulic response at piezometers

25, 26, 27, and 42 (piezometer locations shown in Fig. 1). These piezometers are installed in the shallow aquifer and measured a 1 to 2 m decrease in water level when local dewatering was undertaken to facilitate excavation below the water table (Fig. 8a). The 5 × 7, 8 × 5, and 5 × 9 maps also have a BMU cluster that highlights the distinct hydraulic response at piezometers 35 and 36. In 2021, leakage was observed at the borehole where piezometers 35, 36, and 37 are installed and the borehole was resealed on June 3, 2021. Piezometers 35 and 36 are installed in the intermediate aquifer and measured a sudden increase in head after the borehole was resealed (Fig. 8b). Piezometer 21 also measured an increase in head after the borehole was resealed (Fig. 8b). The 5 × 7, 8 × 5, and 5 × 9 maps also have a BMU cluster highlighting piezometer 21. The BMU clusters with piezometers 21, 35, and 36 are placed close together in the map output, indicating their similarity. These results suggest that SOM clustering can also be used to identify and interpret local anomalies in head data.

Conclusions

The results from SOM clustering of head time series were compared with an existing conceptual model developed through extensive site characterization and visual data inspection. SOM clustering was able to provide insights that are not readily apparent from standard site characterization data analysis and interpretation. The clustering results suggest potential zones with variations in hydraulic connectivity between aquifers, aquifer-scale hydraulic conductivity, and/or recharge influence. Unsupervised SOM analysis can support site characterization by condensing head time series data for simplified visualization and interpretation. This method is well-suited for projects with many piezometers, spatial heterogeneity, and dynamic head changes from groundwater pumping or other stresses. For these types of projects, efficient and insightful data analysis could save time and reduce uncertainty.

We demonstrate how quantization and topographic error measures can help to constrain the selection of different map sizes and shapes. Rather than inspecting many similar maps,

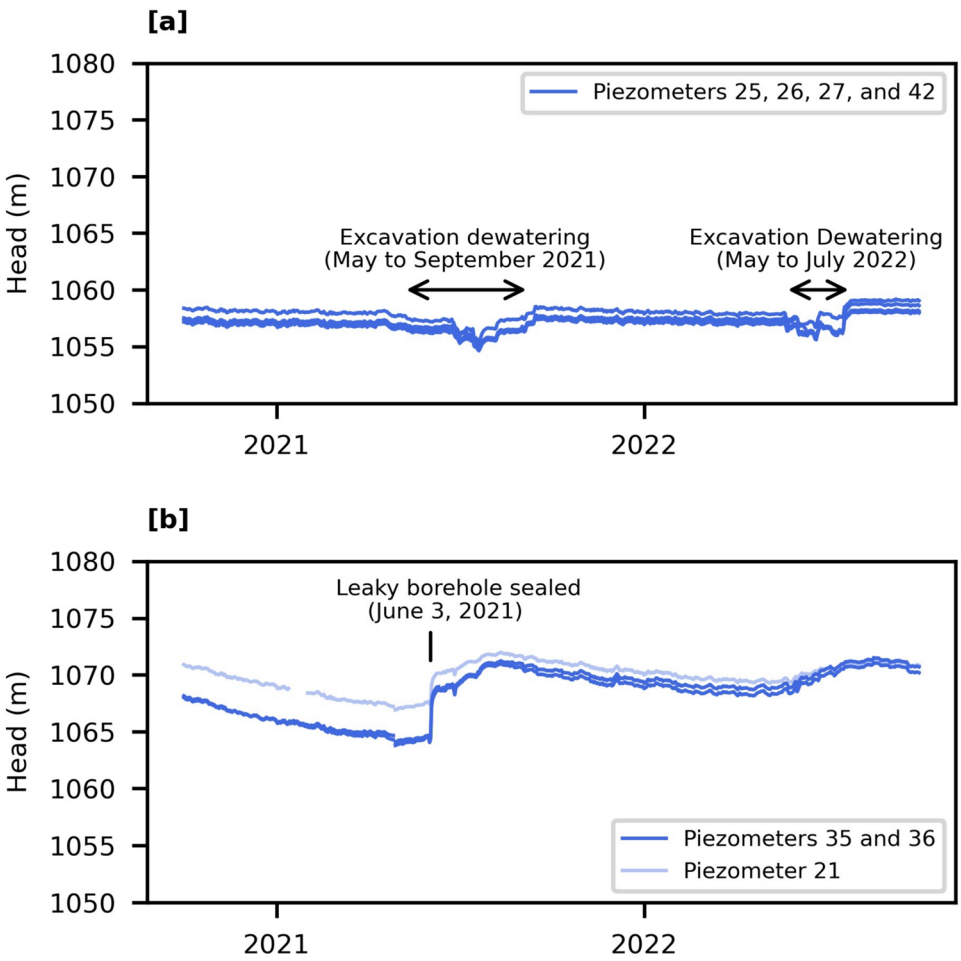

Fig. 8 Piezometers affected by **a** local shallow aquifer dewatering and **b** repair of a leaky borehole

we selected a few different maps that cover the range of quantization and topographic error. Large maps with many nodes are commonly used for SOM applications, but this study demonstrates the value of both small and large map sizes for data exploration and interpretation. Small maps provide simplified visualization and can more easily reveal larger-scale, general patterns like zones within the intermediate aquifer. Large maps can reveal small-scale, more subtle patterns like borehole repair.

SOM analysis is an unsupervised machine learning method, but the results depend on the users' choice of map size and shape and users' interpretation of potential physical meaning. Interpreting the potential physical meaning of SOM clusters results requires general knowledge of geological environments and groundwater flow dynamics. Interpretation at a local site like Red Chris also requires an understanding of site-specific geology, climate, and development activities. Lack of user assumptions and intervention is generally considered an advantage of machine learning methods, but successful practical application requires integration with subject-matter expertise.

Acknowledgements We thank Newmont Corporation and the staff at Red Chris Mine for acquiring and providing data for this research.

Data availability Piezometer data are available in Appendix C of the Red Chris Mine 2022 Groundwater Monitoring Report, which is accessible through the BC Government's Open Information website at http://docs.openinfo.gov.bc.ca/Response_Package_EML-2023-31576.pdf. Raw digital data were provided by Newmont Corporation under a data sharing agreement for the current study. Restrictions apply to use of the raw digital data, so they are available upon reasonable request with permission from Newmont Corporation.

References

Butler JJ, Knobbe S, Reboulet EC, Whittemore DO, Wilson BB, Bohling GC (2021) Water well hydrographs: an underutilized resource for characterizing subsurface conditions. Groundwater 59(6):808–818. https://doi.org/10.1111/gwat.13119

Clark S (2022) Unravelling groundwater time series patterns: visual analytics-aided deep learning in the Namoi region of Australia. Environ Model Softw 149:105295. https://doi.org/10.1016/j.envsoft.2022.105295

Clark S, Sisson SA, Sharma A (2020) Tools for enhancing the application of self-organizing maps in water resources research and engineering. Adv Water Resour 143:103676. https://doi.org/10.1016/j.advwatres.2020.103676

Dramsch JS (2020) 70 years of machine learning in geoscience in review. Adv Geophys 61:1–55. https://doi.org/10.1016/bs.agph.2020.08.002

Kalteh AM, Hjorth P, Berndtsson R (2008) Review of the self-organizing map (SOM) approach in water resources: analysis, modelling and application. Environ Model Softw 23(7):835–845. https://doi.org/10.1016/j.envsoft.2007.10.001

Kohonen T (2001) Self-organizing maps, vol 30. Springer, Berlin Heidelberg. https://doi.org/10.1007/978-3-642-56927-2

Mee E (2024) Self-organizing map analysis of piezometer time series for enhanced aquifer system characterization. MASc thesis, Univ of British Columbia. https://doi.org/10.14288/1.0445489

Mikkelsen E (2002) Cement-bentonite grout backfill for borehole instruments. The Canadian Geotechnical Society. Geotechnical Instrumentation News. https://www.cgs.ca/pdf/GeoTechNews/2002/GIN_Dec2002mikkelsen.pdf Accessed 2024-10-15

Naranjo-Fernández N, Guardiola-Albert C, Aguilera H, Serrano-Hidalgo C, Montero-González E (2020) Clustering groundwater level time series of the exploited Almonte-Marismas Aquifer in southwest Spain. Water 12(4):1063. https://doi.org/10.3390/w12041063

Newcrest Red Chris Mining Limited (2021) Mines Act Annual Reclamation and Environmental Management Act Report for 2020. Newcrest Red Chris Mining Limited, Vancouver, Canada. https://mines.nrs.gov.bc.ca/p/5fa1e42a4635c865df00d57f/docs Accessed 2024–10–15

Newcrest Red Chris Mining Limited (2022) Mines Act Annual Reclamation and Environmental Management Act Report for 2021. Newcrest Red Chris Mining Limited, Vancouver, Canada. https://mines.nrs.gov.bc.ca/p/5fa1e42a4635c865df00d57f/docs Accessed 2024–10–15

Newcrest Red Chris Mining Limited (2023) Mines Act Annual Reclamation and Environmental Management Act Report for 2022. Newcrest Red Chris Mining Limited, Vancouver, Canada. https://mines.nrs.gov.bc.ca/p/5fa1e42a4635c865df00d57f/docs Accessed 2024–10–15

Python Software Foundation (2022) Python—Version 3.9.16 [Computer software]. https://www.python.org/

Rinderer M, van Meerveld HJ, McGlynn BL (2019) From points to patterns: using groundwater time series clustering to investigate subsurface hydrological connectivity and runoff source area dynamics. Water Resour Res 55(7):5784–5806. https://doi.org/10.1029/2018WR023886

Sartirana D, Rotiroti M, Bonomi T, de Amicis M, Nava V, Fumagalli L, Zanotti C (2022) Data-driven decision management of urban underground infrastructure through groundwater-level time-series cluster analysis: the case of Milan (Italy). Hydrogeol J 30(4):1157–1177. https://doi.org/10.1007/s10040-022-02494-5

Sauve M, Shaw B, DeMars S, Dufault D (2023) The integration of geological and hydrogeological models to support design and operations of a tailings facility. In: Goodwill J (eds), Proc, Tailings and Mine Waste 2023, pp 601–612. Accessed 2024-10-15. https://drive.google.com/file/d/1C5dPsnOcksRHrhtkpPZdcGWdt27TRCjg/view?pli=1

Vesanto J, Alhoniemi E (2000) Clustering of the self-organizing map. IEEE Trans Neural Netw 11(3):586–600. https://doi.org/10.1109/72.846731

Vettigli G (2018) MiniSom: minimalistic and NumPy-based implementation of the self organizing map [Computer software]. https://github.com/JustGlowing/minisom/